Pre-Steady-State Kinetic Studies of the Fidelity of Human DNA Polymerase μ[†]

Michelle P. Roettger,[‡,⊥] Kevin A. Fiala,[‡,⊥] Susmitha Sompalli,[‡] Yuxia Dong,[§] and Zucai Suo*[,‡,⊥,§,#,∥]

Department of Biochemistry, Ohio State Biochemistry Program, Ohio State Biophysics Program, Molecular, Cellular, and Developmental Biology Program, and Comprehensive Cancer Center, The Ohio State University, Columbus, Ohio 43210

Received June 11, 2004; Revised Manuscript Received August 16, 2004

ABSTRACT: DNA polymerase μ (Polμ), an X-family DNA polymerase, is preferentially expressed in secondary lymphoid tissues with yet unknown physiological functions. In this study, Polμ was overexpressed in *Escherichia coli* and purified to homogeneity. The purified enzyme had a lifetime of <20 min at 37 °C, but was stable for over 3 h at 25 °C in an optimized reaction buffer. The fidelity of human Polμ was thus determined using pre-steady-state kinetic analysis of the incorporation of single nucleotides into undamaged DNA 21/41-mer substrates at 25 °C. Single-turnover saturation kinetics for all 16 possible deoxynucleotide (dNTP) incorporations and for four matched ribonucleotide (rNTP) incorporations were measured under conditions where Polμ was in molar excess over DNA. The polymerization rate (k_p), binding affinity (K_d), and substrate specificity (k_p/K_d) are 0.006−0.076 s^{-1}, 0.35−1.8 μM, and (8−64) × 10^{-3} μM^{-1} s^{-1}, respectively, for matched incoming dNTPs, (2−30) × 10^{-5} s^{-1}, 7.3−135 μM, and (4−61) × 10^{-7} μM^{-1} s^{-1}, respectively, for mismatched incoming dNTPs, and (2−73) × 10^{-4} s^{-1}, 45−302 μM, and (7−1300) × 10^{-7} μM^{-1} s^{-1}, respectively, for matched incoming rNTPs. The overall fidelity of Polμ was estimated to be in the range of 10^{-3}−10^{-5} for both dNTP and rNTP incorporations and was sequence-independent. The sugar selectivity, defined as the substrate specificity ratio of a matched dNTP versus a matched rNTP, was measured to be in the range of 492−10959. In addition to a slow and distributive DNA polymerase activity, Polμ was identified to possess a weak strand-displacement activity. The potential biological roles of Polμ are discussed.

DNA polymerase μ (Polμ)[1] (*1*, *2*) is a recently identified member of the X-family DNA polymerases. This family includes terminal deoxynucleotidyl transferase (TdT), DNA polymerase β (Polβ), and DNA polymerase λ (Polλ). Polβ is a DNA repair polymerase involved in base excision repair in eukaryotes (*3*, *4*). Human Polλ has 54% homology to human Polβ (identity 34%) (*1*). The biological functions of Polλ are not yet explicitly clear, although Polλ is proposed to function in meiosis (*5*) and base excision repair (*6*). The Polλ-deficient mice display hydrocephalus, situs inversus, chronic sinusitis, and male infertility (*7*). Meanwhile, TdT has been shown to catalyze nucleotide additions in a template-independent manner, and its expression is restricted to primary lymphoid tissues (*8*). TdT contributes to the diversification of immunoglobulin (Ig) and antigen receptors by adding nontemplated nucleotides to the V−D and D−J junctions of Ig and T-cell receptor genes during V(D)J recombination (*8*).

Among the X-family polymerases, Polμ is most homologous to TdT. A comparison of the human forms of these enzymes reveals 41% amino acid sequence identity (*1*, *2*). Sequence alignment analysis and biochemical studies indicate that the C termini of Polμ, TdT, and Polλ form Polβ-like domains (*9*, *10*). In addition to the Polβ-like domain, each of the three polymerases contains an N-terminal BRCT domain (*1*, *2*, *9*). This BRCT domain likely mediates protein−protein and DNA−protein interactions, thus playing a role in modulation of polymerase activity and shaping the protein's cellular function (*11*, *12*). Preferential expression in secondary lymphoid organs as well as the observed low fidelity of Polμ has led to the hypothesis that this enzyme is an error-prone mutase, active in somatic hypermutation (*9*). The presence of Polμ in the absence of TdT in germinal center B cells, the low levels of Polμ expression in thymus and bone marrow, and the intrinsic terminal transferase activity possessed by Polμ in the presence of Mn^{2+} all suggest that this enzyme may play a role in V(D)J recombination, thereby complementing the biological functions of TdT (*9*). Moreover, the basal expression of Polμ in most tissues suggests a potential role in the nonhomologous end-joining pathway (NHEJ) for general repair of DNA double-strand breaks (DSBs). NHEJ is a major pathway for repair of DSBs introduced by exogenous sources, including oxida-

[†] This work was supported in part by American Chemical Society Petroleum Research Fund Grant PRF38364-G4, by American Cancer Society Grant IRG-98-278-03, and by TriLink Biotechnologies Research Funding Program to Z.S. Both M.P.R. and K.A.F. were supported by the National Institutes of Health Chemistry and Biology Interface Program at the Ohio State University (Grant T32 GM08512-08).

* Author to whom correspondence should be addressed [telephone (614) 688-3706; fax (614) 292-6773; e-mail suo.3@osu.edu].

[‡] Department of Biochemistry.

[⊥] Ohio State Biochemistry Program.

[§] Ohio State Biophysics Program.

[#] Molecular, Cellular, and Developmental Biology Program.

[∥] Comprehensive Cancer Center.

[1] Abbreviations: BSA, bovine serum albumin; dNTP, 2′-deoxynucleoside 5′-triphosphate; rNTP, ribonucleoside 5′-triphosphate; DSB, DNA double-strand break; DTT, dithiothreitol; Ig, immunoglobulin; Polβ, DNA polymerase beta; Polλ, DNA polymerase lambda; Polμ, DNA polymerase mu; NHEJ, nonhomologous end-joining pathway; TBE, Tris/borate/EDTA electrophoresis buffer; TdT, terminal deoxynucleotidyl transferase.

10.1021/bi048782m CCC: $27.50
Published on Web 10/08/2004

tion and ionizing radiation in all cell types, and is an essential mechanism that repairs DSBs during V(D)J recombination (*13*). The proposed role of Polμ in NHEJ and V(D)J recombination is substantiated by the following *in vitro* observations: Polμ and TdT form essentially identical complexes with the end-joining factors Ku and the XRCC4−ligase IV complex (*14*), and Polμ promotes microhomology searching and pairing to realign primers with terminal mismatches by looping out any mismatched template nucleotides (*15*). Recently, Polμ, like TdT, was shown to incorporate both rNTPs and dNTPs using either DNA or RNA primers (*16*, *17*). Additionally, Polμ can also bypass several DNA lesions, including *cis-syn* thymidine−thymidine dimers, abasic sites, 8-oxoguanines, 1, N^6-ethenoadenines, *N*-2-acetylaminoflourines, (+)- and (−)-*trans-anti*-benzo[*a*]-pyrene-N^2-dG adducts, and platinum DNA adducts, through a deletion mechanism (*18*, *19*). The lesion bypass ability of Polμ indirectly supports the proposed mutase role of this polymerase in somatic hypermutation.

To evaluate the hypothesis that regards Polμ as a mutase in immunoglobulin (Ig) maturation, we used pre-steady-state kinetic methods to accurately measure the fidelity of human Polμ based on all 16 possible dNTP incorporations and four matched rNTP incorporations into normal DNA primer/template substrates. In addition to the measurement of nucleotide incorporation fidelity, the sugar selection fidelity of Polμ was also determined. The potential biological functions of Polμ are discussed on the basis of our pre-steady-state kinetic data.

MATERIALS AND METHODS

Reagents. [γ-^{32}P]ATP was purchased from Perkin-Elmer Life Sciences (Boston, MA); dNTPs were purchased from Gibco-BRL (Rockville, MD) and rNTPs from TriLink Biotechnologies (San Diego, CA). Calf intestine alkaline phosphatase was from Fermentas (Hanover, MD) and T4 polynucleotide kinase from USB (Cleveland, OH). Biospin columns were from Bio-Rad Laboratories (Hercules, CA), and activated calf thymus DNA was from Sigma-Aldrich (St. Louis, MO). All synthetic oligonucleotides used in DNA substrate preparation were provided by TriLink Biotechnologies.

Cloning and Purification of Full-Length Human Polμ. Human Polμ was subcloned into the *Nde*I/*Xho*I sites of the vector pET28b from a previously published plasmid pEGUh6-POLM provided by Dr. Z. Wang (*15*). The constructed plasmid pET28b-Polμ was transformed into *E. coli* strain BL21-CodonPlus(DE3)-RIL (Stratagene) to express human Polμ fused to both N- and C-terminal His_6 tags. Transformed *E. coli* cells were grown at 37 °C in the presence of 40 μg/mL kanamycin and 25 μg/mL chloramphenicol until reaching an OD_{600} of 0.55. At this point, the cultures were induced with 0.1 mM IPTG and incubated at 18 °C for 15 h. Cells were harvested (4000 rpm, 15 min) and resuspended in buffer A (10 mM $KHPO_4$, pH 7.0, 0.5 M NaCl, 10 mM $MgCl_2$, 10% glycerol, 0.1% β-mercaptoethanol, 5 mM imidazole). After the addition of 1 mM PMSF and one tablet of protease inhibitor cocktail (Roche), resuspended cells were lysed by French press. The resulting lysate was cleared by ultracentrifugation (35000 rpm, 40 min). The supernatant was pooled and incubated overnight at 4 °C with nickel-NTA superflow resin (Qiagen). The supernatant was removed by centrifugation in a swing-bucket centrifuge (2500 rpm, 10 min), and the Polμ-bound nickel resin was subsequently packed into a column. Bound proteins were eluted through a linear gradient of 20−500 mM imidazole in buffer B (10 mM $KHPO_4$, pH 7.0, 0.35 M NaCl, 2.5 mM $MgAc_2$, 10% glycerol, 0.1% 2-mercaptoethanol). Polμ-containing fractions were pooled and dialyzed against 2 L of buffer C (10 mM $KHPO_4$, pH 7.0, 0.25 M NaCl, 10% glycerol, 1 mM EDTA, 0.1% β-mercaptoethanol) at 4 °C. The dialyzed protein solution was loaded into a prepacked ssDNA−cellulose column (Sigma). After washing, Polμ was then eluted with 250−1000 mM NaCl gradient in buffer C. The fractions containing Polμ were pooled and dialyzed against buffer D (25 mM HEPES, pH 7.5, 200 mM NaCl, 10% glycerol, 1 mM EDTA, 0.1% β-mercaptoethanol). The dialyzed Polμ was passed through a 10 mL DEAE-Sepharose column (Amersham Pharmacia Biotech). The eluate was applied to a MonoS column (Amersham Pharmacia Biotech) and eluted using a gradient of 200−1000 mM NaCl in buffer D. Fractions containing Polμ were pooled, dialyzed against buffer D, and concentrated using a Centriprep YM-30 (Millipore). The concentrated protein was ultimately dialyzed against buffer E (25 mM HEPES, pH 7.5, 200 mM NaCl, 10% glycerol, 1 mM EDTA, 1 mM DTT, 50% glycerol). Polμ was purified to >95% purity based on SDS−PAGE analysis (Figure 1). The concentration of the purified Polμ was measured spectrophotometrically at 280 nm using the calculated extinction coefficient of 52 857 M^{-1} cm^{-1}. The sequence of the purified Polμ was confirmed by in-gel trypsin digestion and capillary−liquid chromatography−nanospray tandem mass spectrometry analysis (nano-LC/MS/MS) at the Campus Chemical Instrument Center at The Ohio State University.

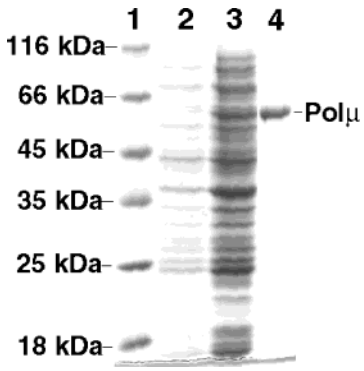

FIGURE 1: Expression and purification of human Polμ. Coomassie Blue staining and SDS−PAGE analysis of purified human Polμ are shown: (lane 1) protein size marker; (lane 2) crude extracts of noninduced cells; (lane 3) crude extracts of IPTG-induced cells; (lane 4) purified full-length human Polμ.

DNA Oligomers. To prepare DNA substrates for dNTP incorporation assays, a 21-mer primer was annealed to each of four different 41-mer templates (Table 1). These oligomers were purified by denaturing polyacrylamide gel electrophoresis (18% acrylamide, 8 M urea), and their concentrations were determined by UV absorbance at 260 nm with the following extinction coefficients: 21-mer, ϵ = 194 100 M^{-1} cm^{-1}; D-1 41-mer, ϵ = 397 600 M^{-1} cm^{-1}; D-6 41-mer, ϵ = 394 200 M^{-1} cm^{-1}; D-7 41-mer, ϵ = 392 200 M^{-1} cm^{-1}; D-8 41-mer, ϵ = 389 500 M^{-1} cm^{-1}. The 21-mer primer was 5′-^{32}P-labeled by incubation with [γ-^{32}P]ATP and

Table 1: DNA Substrates

D-1	5′-CGCAGCCGTCCAACCAACTCA 3′-GCGTCGGCAGGTTGGTTGAGTAGCAGCTAGGTTACGGCAGG-5′
D-6	5′-CGCAGCCGTCCAACCAACTCA 3′-GCGTCGGCAGGTTGGTTGAGTGGCAGCTAGGTTACGGCAGG-5′
D-7	5′-CGCAGCCGTCCAACCAACTCA 3′-GCGTCGGCAGGTTGGTTGAGTTGCAGCTAGGTTACGGCAGG-5′
D-8	5′-CGCAGCCGTCCAACCAACTCA 3′-GCGTCGGCAGGTTGGTTGAGTCGCAGCTAGGTTACGGCAGG-5′
D-8g*	5′-CGCAGCCGTCCAACCAACTCA CGTCGATCCAATGCCGTCC-3′ 3′-GCGTCGGCAGGTTGGTTGAGTCGCAGCTAGGTTACGGCAGG-5′

*****The downstream 19-mer primer was 5′-phosphorylated. The top strand was composed of two oligonucleotides (21- and 19-mer) with a single-nucleotide gap between them.

T4 polynucleotide kinase at 37 °C for an hour. Subsequent centrifugation through a Biospin-6 column served to remove any remaining [γ-^{32}P]ATP from the newly labeled 21-mer mixture. Both the 21-mer and 41-mer (1:1.1 molar ratio) were annealed to form a 21/41-mer complex by heating the mixture at 95 °C for 10 min and then slowly cooling it to room temperature. Single-nucleotide gapped DNA was prepared in the same manner with 21-mer, 19-mer, and 41-mer annealed at a 1:2:2 molar ratio, respectively.

Reaction Buffer Optimization. Using a rapid chemical quench apparatus (KinTek, Clarence, PA) (*20*), a preincubated solution of 40 nM 5′-radiolabeled D-1 and 200 nM Polμ was mixed with 100 μM dTTP to initiate the reaction. The reactions were quenched by the addition of 0.37 M EDTA at various time intervals. For optimization reactions that were too slow to be efficiently performed using the rapid chemical quench, assays were carried out manually. In the latter case, an aliquot of the reaction mixture (10 μL) was withdrawn after various times and quenched with 0.37 M EDTA (40 μL). The NaCl optimization buffer consisted of 50 mM HEPES (pH 7.5 at 37 °C), 10 mM $MgCl_2$, 0.2 mM EDTA, 5 mM DTT, 0.1 mg/mL BSA, 10% glycerol, and various concentrations of NaCl ranging from 12 to 432 mM. The $MgCl_2$ optimization buffer consisted of 50 mM HEPES (pH 7.5 at 37 °C), no additional NaCl, 0.2 mM EDTA, 5 mM DTT, 0.1 mg/mL BSA, 10% glycerol, and various concentrations of $MgCl_2$ ranging from 2.5 to 50 mM. The pH optimization buffer consisted of 8.75 mM $MgCl_2$, no additional NaCl, 0.2 mM EDTA, 5 mM DTT, 0.1 mg/mL BSA, 10% glycerol, and either 25 mM MES−NaOH for pH 6.0, 25 mM HEPES for pH 6.8−9.0, or 25 mM glycine−NaOH buffer for pH 10.0 at 37 °C.

Reaction Buffer M. The optimized reaction buffer M consists of 50 mM HEPES (pH 7.8 at 37 °C and pH 8.0 at 25 °C), 12 mM NaCl, 8.75 mM $MgCl_2$, 0.2 mM EDTA, 5 mM DTT, 0.1 mg/mL BSA, and 10% glycerol. Unless noted otherwise, all concentrations reported in this paper refer to final concentrations after mixing.

Enzyme Stability Assays. To assess the stability of Polμ, solutions containing 30 nM 5′-^{32}P-labeled D-1 and 150 nM Polμ in buffer M were incubated at either 25 or 37 °C for various periods of time. After times ranging from 10 min to 3 h, an aliquot of the incubated mixture was withdrawn and mixed with 100 μM dTTP. One minute after reaction initiation with dTTP, each corresponding reaction mixture (10 μL) was quenched with 0.37 M EDTA (40 μL). Quenched reactions were then separated and analyzed (see Product Analysis).

Measurement of the Substrate Specificity of an Incoming Nucleotide. A solution of 150 nM Polμ and 30 nM 5′-^{32}P-labeled D-1 (or D-6, D-7, or D-8) was preincubated in buffer M for 5 min at 25 °C. Nucleotide incorporation was initiated by the addition of increasing concentrations of dNTP (0.25−300 μM) to the reaction mixture. Each reaction (10 μL) was manually quenched with 0.37 M EDTA (40 μL) at specific time points ranging from 6 to 600 s for correct incoming nucleotide and from 3 min to 3 h for an incorrect incoming nucleotide. The reactions were subsequently analyzed as described below.

Product Analysis. All reaction products were separated by denaturing polyacrylamide gel electrophoresis (17% acrylamide, 8 M urea) in 1× TBE running buffer. Products and unreacted primer were subsequently detected and quantitated using a PhosphorImager 445 SI and ImageQuant software (Molecular Dynamics, Sunnyvale, CA).

DNA Trap Experiment. To qualitatively confirm distributive DNA polymerization by Polμ, a preincubated solution of 100 nM Polμ and 100 nM D-8 (Table 1) in buffer M were rapidly mixed with a solution containing both 100 μM dNTPs and 2.44 mg/mL activated calf thymus trap DNA. The reaction was quenched after 30 min in 0.37 M EDTA before polyacrylamide gel separation under conditions described above (see Product Analysis).

Data Analysis. All data were fit by nonlinear regression using KaleidaGraph software (Synergy Software, Reading, PA). The concentration of products was plotted against reaction time and the resulting time course fit to a single-exponential equation: $[\text{product}] = A[1 - \exp(-k_{obs}t)]$, where A represents the initial concentration of the binary enzyme•DNA complex and k_{obs} represents the observed single-turnover rate.

The observed single-turnover rates were subsequently plotted against their corresponding nucleotide concentrations, and the data were fit to the hyperbolic equation $k_{obs} = k_p[\text{dNTP}]/(K_d + [\text{dNTP}])$ to obtain the equilibrium dissociation constant, K_d, and the maximum incorporation rate, k_p.

Data from the [α-^{32}P]dNTP incorporation experiment in the absence of trap dNTP (nonradioactive) were fit to a burst equation (*21*−*23*), $[\text{product}] = \{[k_p k_1 t/(k_p + k_1)] + [k_p/(k_p + k_1)]^2\{1 - \exp[-(k_p + k_1)t]\}\}[E_0]$, to obtain the DNA dissociation rate constant, k_1, and the observed nucleotide incorporation rate constant, k_p. $[E_0]$ is the initial enzyme active site concentration.

RESULTS

Protein Purification. Although human DNA Polμ (494 amino acid residues and 55.9 kDa) has been reported previously to be overexpressed in *E. coli* strains BL21(DE3) (*1*) and BL21(DE3) pLysS (*2*), we failed to achieve clear induction of this protein using IPTG in these strains under various conditions including different induction temperatures, induction times, and IPTG concentrations. Fortunately, human DNA Polμ can be overexpressed in *E. coli* strain BL21-CodonPlus(DE3)-RIL (or RP) by inducing with 0.1 mM IPTG at 18 °C (Figure 1). The codon usage in human Polμ could cause its undetectable expression in *E. coli* BL21-(DE3): 13 of 44 arginine codons of human Polμ are rare

(AGA/AGG) (*24*). Similar results have been found in the expression of murine TdT in *E. coli* (*25*). Following the published reports (*1*, *2*, *15*), we added a hexahistidine tag to the N and C termini of Polμ for the convenience of protein purification. Polμ was purified to >95% purity (Figure 1) through nickel-NTA, ssDNA−cellulose, DEAE-Sepharose, and MonoS columns (see Materials and Methods). The yield was ~0.5 mg/L of initial *E. coli* culture. The sequence of the N-terminal 139 amino acid residues of the purified Polμ was confirmed by in-gel trypsin digestion and nano-LC/MS/MS analysis (see Materials and Methods). The hexahistidine tags of the purified Polμ were also detected by Western blot analysis using an anti-hexahistidine tag antibody (data not shown).

Reaction Buffer Optimization. Enzyme activity is affected significantly by the presence and identities of components, the concentration of each component, and the pH of a reaction buffer in an *in vitro* system. An optimal reaction buffer will allow a polymerase to incorporate nucleotides with maximum polymerization rate and full reaction amplitude. To optimize the reaction buffer, $MgCl_2$ concentration, NaCl concentration, and pH were individually varied while the concentrations of all other buffer components remained fixed. Each of the optimization reactions was initiated by mixing a preincubated solution of 40 nM 5′-radiolabeled D-1 primer/template (Table 1) and 200 nM Polμ with 100 μM dTTP in buffer at 37 °C. The reaction was quenched by 0.37 M EDTA at various time intervals. Experiments were accomplished either manually or by using a rapid chemical quench apparatus (see Materials and Methods). The optimized reaction buffer M was determined to contain 12 mM NaCl (Figure 2A) and 8.75 mM $MgCl_2$ (Figure 2B) and to have a pH of 7.8 at 37 °C (Figure 2C). In the pH optimization experiments, three different buffers were used to cover a large pH range. To help stabilize the enzyme in these reactions, 0.1 mg/mL BSA and 10% glycerol were also included in the optimized reaction buffer M (see Materials and Methods).

Enzyme Stability Assays. A relatively slow rate of nucleotide incorporation observed in the optimization assays indicated that in order to accurately ascertain the fidelity of Polμ, we needed this enzyme to retain its full activity over a span of several hours. To determine whether the recombinant Polμ was fully active at 37 °C for the desired length of time in buffer M, enzyme stability assays were conducted. A solution of 30 nM D-1 and 150 nM Polμ in buffer M was incubated at 37 °C. After incubation time intervals ranging from 0 to 200 min, 10 μL of the enzyme−DNA solution was withdrawn and mixed with 100 μM dTTP to initiate the reaction. Each reaction was stopped after exactly 1 min (~$7t_{1/2}$) at 37 °C, which was sufficient time to allow a single turnover of dTTP incorporation to be completed (see below). If the enzyme remains stable during incubation, the product concentration would be expected to reach full reaction amplitude (~30 nM) for all incubation periods. Surprisingly, the product formation began to drop dramatically after only 20 min of incubation at 37 °C (Figure 3). This suggested that the purified Polμ would not be stable long enough to complete the slow incorrect dNTP incorporation assays at 37 °C. To achieve greater stability of this enzyme over a greater period of time, we lowered the incubation temperature and conducted the same enzyme stability assay at 25 °C. Interestingly, the product concentration remained close to full amplitude (equal to the initial E·DNA concentration) over 3 h at this temperature (Figure 3). In addition, we performed the similar enzyme stability assay with a 5-fold molar excess of D-1 over Polμ (data not shown), and the product formation patterns were similar to those shown in

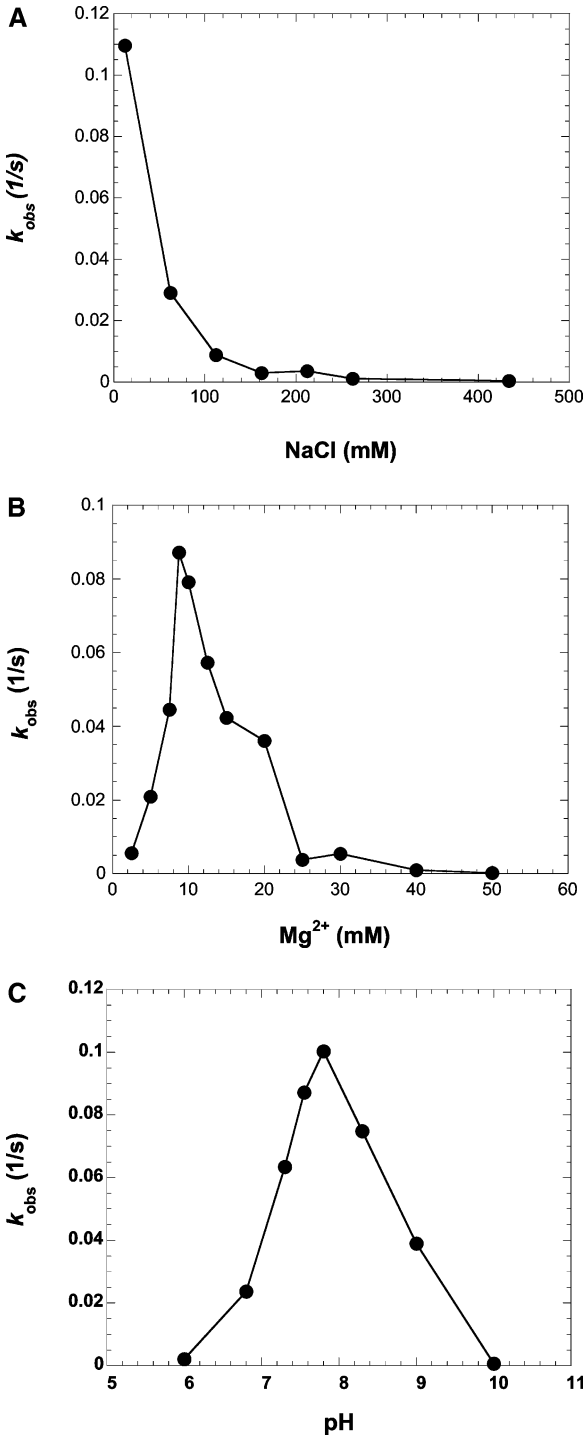

FIGURE 2: Reaction buffer optimization. The optimal levels of $MgCl_2$ concentration, NaCl concentration, and buffer pH were examined under single-turnover conditions at 37 °C by rapidly mixing 100 μM correct nucleotide dTTP with a preincubated solution of 40 nM D-1 and 200 nM Polμ. (A) The NaCl concentration was varied from 12 to 432 mM. (B) The $MgCl_2$ concentration was varied from 2.5 to 50 mM. (C) The pH of the reaction buffer was varied from 6.0 to 10.0. Single-turnover rates were measured in 25 mM MES−NaOH buffer for pH 6.0, in 25 mM HEPES buffer for pH 7.0−9.0, and in 25 mM glycine−NaOH buffer for pH 10.0.

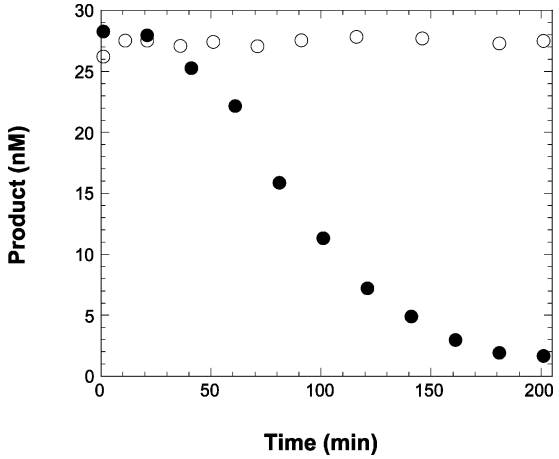

FIGURE 3: Polμ stability assay. Solution containing 30 nM D-1 preincubated with 150 nM Polμ in optimized reaction buffer M was incubated at either 25 °C (○) or 37 °C (●). Aliquots were withdrawn after various incubation times ranging from 10 to 200 min and reacted with 100 μM dTTP for 1 min at 37 °C before being quenched by 0.37 M EDTA. The product concentration was plotted against the incubation time.

Scheme 1

$$E{\bullet}DNA_n + dNTP \underset{k_{off}}{\overset{k_{on}}{\rightleftharpoons}} E{\bullet}DNA_n{\bullet}dNTP \overset{k_p}{\rightleftharpoons} E{\bullet}DNA_{n+1}{\bullet}PPi \overset{k_1}{\rightleftharpoons} E + DNA_{n+1} + PPi$$

Figure 3. Therefore, all subsequent nucleotide incorporation assays were performed at 25 °C.

Rapid Equilibrium of Nucleotide Binding to the Binary Complex of Enzyme and DNA. Scheme 1 is a proposed kinetic mechanism for single-nucleotide incorporation into a synthetic primer/template substrate catalyzed by Polμ. This minimal mechanism is shared by all DNA polymerases that have been studied so far (*23*, *26*−*33*) including two other X-family members, Polβ (*29*) and Polλ (*23*). In Scheme 1, the initially formed binary complex of enzyme and DNA (E·DNA$_n$) binds an incoming nucleotide (dNTP) to form a ternary complex E·DNA$_n$·dNTP. During catalysis, the DNA primer is elongated by one nucleotide, pyrophosphate (PPi) is produced, and the product-containing ternary complex, E·DNA$_{n+1}$·PPi, is then formed. After catalysis, the enzyme dissociates from E·DNA$_{n+1}$·PPi to initiate subsequent turnovers. Scheme 1 sets up a kinetic basis for evaluating substrate selection in a template-directed polymerization event catalyzed by Polμ.

To measure the binding affinity of an incoming nucleotide in Scheme 1, the binding (k_{on}) and dissociation (k_{off}) steps have to be much faster than the nucleotide incorporation (k_p), such that the reversible binding of dNTP is at rapid equilibrium. To verify this rapid equilibrium, a preincubated solution of Polμ, 5-fold unlabeled D-8, and [α-^{32}P]dGTP (20 μM) in the optimized buffer M lacking Mg^{2+} and containing EDTA (1 mM) was mixed with a solution of excess unlabeled dGTP (2 mM) and Mg^{2+} (9.75 mM) for various reaction times prior to being quenched with EDTA. Although Polμ was purified and stored in the absence of divalent metal ions, we used additional 1 mM EDTA present in the preincubated E·DNA·[α-^{32}P]dNTP solution to chelate any contaminant divalent cations carried over from the protein purification. This concentration of EDTA was shown to be sufficient to prevent any product formation in this preincubated solution (data not shown). If the dissociation of [α-^{32}P]-dNTP from the E·DNA·[α-^{32}P]dNTP ternary complex was much faster than the polymerization, we would expect to see very little α-^{32}P-labeled product formation due to the unfavorable kinetic partitioning and large molar excess of unlabeled dGTP that would trap dissociated [α-^{32}P]dNTP. This assay resulted in a time course (●) showing background-level radiolabeled product (<0.01 nM at the longest reaction time in Figure 4). This suggested the nucleotide dissociation rate constant was indeed much faster than the polymerization rate constant ($k_{off} \gg k_p$). In addition, the product concentration was significantly less when compared to a similar experiment performed with truncated Polλ in which k_{off} is determined to be 300 s^{-1} (*23*). We therefore placed a lower limit on the dissociation rate constant of dGTP from Polμ·DNA to be >300 s^{-1}. In addition, the affinity of dGTP (K_d) was measured to be 1.8 μM (Table 2). The association rate constant of the binding of dGTP to the Polμ·D-8 binary complex, $k_{on} = k_{off}/K_d > 1.7 \times 10^8$ M^{-1} s^{-1}, was thus calculated from the values of k_{off} and K_d. This suggested the binding of a nucleotide to the binary complex Polμ·DNA was under diffusion control or at rapid equilibrium.

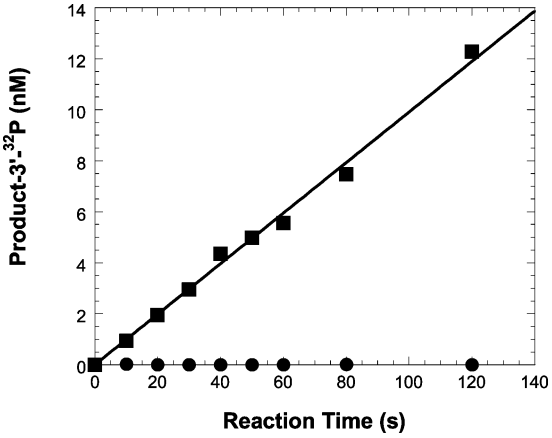

FIGURE 4: Incorporation of [α-^{32}P]dGTP into D-8. In the first time course, a preincubated solution of Polμ (60 nM), unlabeled D-8 (300 nM), [α-^{32}P]dGTP (20 μM), and 1 mM EDTA in the absence of Mg^{2+} was reacted with a solution containing a large molar excess of unlabeled dGTP (2 mM) and Mg^{2+} (9.75 mM) for various reaction times (●). In the second time course, a preincubated solution of Polμ (60 nM), unlabeled D-8 (300 nM), [α-^{32}P]dGTP (20 μM), and 1 mM EDTA in the absence of Mg^{2+} was reacted with a solution containing Mg^{2+} (9.75 mM) with no additional unlabeled dGTP for various reaction times (■).

Rapid DNA Dissociation and Slow Polymerization. The lack of product formation shown above could be due to preincubation of the E·DNA·dNTP ternary complex in the absence of Mg^{2+}. To ensure this not the case, we performed another control experiment. In this experiment, a preincubated solution of Polμ (60 nM), unlabeled D-8 (300 nM), [α-^{32}P]dGTP (20 μM), and EDTA (1 mM) in the optimized buffer lacking Mg^{2+} was mixed with a solution containing Mg^{2+} and no additional unlabeled trap dGTP for various reaction times. This experiment yielded a time course of product formation (■) (Figure 4) that was similar to that obtained when a preincubated Polμ·DNA binary complex in the presence of Mg^{2+} reacted with dNTP·Mg^{2+} (data not shown). This suggested the nucleotide incorporation was not affected by preincubating the E·DNA·dNTP ternary complex in the absence of Mg^{2+}. Moreover, the lack of a burst phase in the data (■) suggested the k_1 value was significantly larger

Table 2: Pre-Steady-State Kinetic Parameters of Human DNA Polμ

nucleotide	K_d (μM)	k_p (s^{-1})	k_p/K_d (μM^{-1} s^{-1})	fidelity[a]	sugar selectivity[b]
		Template A (D-1)			
dTTP	1.4 ± 0.1	$7.6 \times 10^{-2} \pm 1 \times 10^{-3}$	5.6×10^{-2}	1	2074
rUTP	86 ± 10	$2.3 \times 10^{-3} \pm 9 \times 10^{-5}$	2.7×10^{-5}	4.8×10^{-4}	
dATP	80 ± 8	$9.7 \times 10^{-5} \pm 4 \times 10^{-6}$	1.2×10^{-6}	2.2×10^{-5}	
dCTP	98 ± 24	$3.0 \times 10^{-4} \pm 3 \times 10^{-5}$	3.0×10^{-6}	5.5×10^{-5}	
dGTP	81 ± 21	$7.4 \times 10^{-5} \pm 7 \times 10^{-6}$	9.1×10^{-7}	1.6×10^{-5}	
		Template G (D-6)			
dCTP	0.35 ± 0.03	$2.2 \times 10^{-2} \pm 4 \times 10^{-4}$	6.4×10^{-2}	1	492
rCTP	56 ± 13	$7.3 \times 10^{-3} \pm 5 \times 10^{-4}$	1.3×10^{-4}	2.0×10^{-3}	
dATP	89 ± 11	$6.1 \times 10^{-5} \pm 3 \times 10^{-6}$	6.9×10^{-7}	1.1×10^{-5}	
dGTP	12 ± 3	$4.0 \times 10^{-5} \pm 2 \times 10^{-6}$	3.3×10^{-6}	5.2×10^{-5}	
dTTP	51 ± 11	$3.7 \times 10^{-5} \pm 3 \times 10^{-6}$	7.1×10^{-7}	1.1×10^{-5}	
		Template T (D-7)			
dATP	0.76 ± 0.34	$6.1 \times 10^{-3} \pm 5 \times 10^{-4}$	8.0×10^{-3}	1	10959
rATP	302 ± 24	$2.2 \times 10^{-4} \pm 7 \times 10^{-6}$	7.3×10^{-7}	9.1×10^{-5}	
dCTP	24 ± 10	$1.5 \times 10^{-4} \pm 1 \times 10^{-5}$	6.1×10^{-6}	7.6×10^{-4}	
dGTP	7.3 ± 1.5	$3.0 \times 10^{-5} \pm 1 \times 10^{-6}$	4.1×10^{-6}	5.1×10^{-4}	
dTTP	45 ± 7	$2.3 \times 10^{-5} \pm 1 \times 10^{-6}$	5.0×10^{-7}	6.3×10^{-5}	
		Template C (D-8)			
dGTP	1.8 ± 0.5	$5.5 \times 10^{-2} \pm 3 \times 10^{-3}$	3.0×10^{-2}	1	6122
rGTP	45 ± 7	$2.2 \times 10^{-4} \pm 8 \times 10^{-6}$	4.9×10^{-6}	1.6×10^{-4}	
dATP	90 ± 30	$5.3 \times 10^{-5} \pm 8 \times 10^{-6}$	6.0×10^{-7}	2.0×10^{-5}	
dCTP	135 ± 28	$2.8 \times 10^{-4} \pm 3 \times 10^{-5}$	2.1×10^{-6}	6.7×10^{-5}	
dTTP	97 ± 14	$3.6 \times 10^{-5} \pm 2 \times 10^{-6}$	3.7×10^{-7}	1.2×10^{-5}	

[a] Calculated as $(k_p/K_d)_{incorrect}/[(k_p/K_d)_{correct} + (k_p/K_d)_{incorrect}]$. [b] Calculated as $(k_p/K_d)_{dNTP}/(k_p/K_d)_{rNTP}$.

than the k_p value (*21*, *22*). We attempted to fit the data (■) to a burst equation (see Data Analysis under Materials and Methods) to obtain observed k_p and k_1 (Scheme 1) as we have done previously with Polλ (*23*), but failed due to lack of convergence of nonlinear regression analysis. Further kinetic experiments to determine these rate constants are under way in our laboratory.

Substrate Specificity of Incoming Correct dNTP. The lack of a burst phase in the time course of product formation (■) in Figure 4 suggested the observed reaction rate was not the true nucleotide incorporation rate in the first turnover and was complicated by the fast dissociation of the enzyme and DNA binary complex (E·DNA) (*22*). To eliminate the complication from subsequent turnovers, we measured the true nucleotide incorporation rate under single-turnover conditions. These single-turnover experiments were performed with the enzyme in molar excess over DNA to allow the direct observation of the conversion of 21/41-mer to 22-mer/41-mer in a single pass of D-1 through the enzymatic pathway (*22*). Solutions of 30 nM radiolabeled D-1 and 150 nM Polμ were incubated at 25 °C in buffer M and then reacted with increasing concentrations of the correct incoming nucleotide, dTTP. Aliquots of the reactions were quenched with EDTA at various time intervals. The products were separated from unextended 21-mer primer by gel electrophoresis and the results quantitated using PhosphorImaging technology. The concentration of product was plotted against time, and the data were fit to a single-exponential equation to obtain an observed single turnover rate, k_{obs}, for each concentration of dTTP (Figure 5A). The reaction amplitudes achieved were close to 100% in all time courses. These reaction amplitudes were not improved with a larger excess of Polμ over DNA (data not shown). This suggested that the 5-fold excess of enzyme over DNA was enough to ensure that nearly all DNA 21/41-mer molecules were bound by the enzyme. The single-turnover rates were then plotted against dTTP concentration, and the curve was fit to a hyperbolic equation (see Materials and Methods) to obtain a dissociation constant (K_d) of 1.4 ± 0.1 μM and a maximum rate of polymerization (k_p) of 0.076 ± 0.001 s^{-1} at 25 °C (Figure 5B).

Similar single-turnover experiments for the remaining correct nucleotide incorporations were performed with dCTP incorporation against D-6, dATP incorporation against D-7, and dGTP incorporation against D-8 at 25 °C. The measured values of K_d and k_p are listed in Table 2. The substrate specificity of the incorporation of each correct nucleotide, defined by pre-steady-state kinetics as k_p/K_d (*22*), was calculated, and the values determined are given in Table 2.

Substrate Specificity of Incoming Incorrect dNTP. To evaluate if Polμ also incorporated incorrect nucleotides, we tested all 12 possible mismatched dNTP incorporations into D-1, D-6, D-7, and D-8 (Table 1). With a reaction time of 3 h, all possible misincorporations did occur (Figure 6A). To determine the incorporation fidelity of Polμ, we used the same assay described above to determine the substrate specificity of each misincorporation (data not shown). The corresponding kinetic parameters are recorded in Table 2. Due to weak binding affinity and slow misincorporation, the substrate specificity for an incorrect dNTP was 3−5 orders of magnitude lower than the value of a correct nucleotide. The observed tighter binding of mismatched dGTP to the enzyme·D-7 complex ($K_d = 7.3$ μM) when compared to other mismatched base pairs is likely due to the formation of relatively stable G:T wobble base pair. In addition, the misincorporation of dCTP into D-1, D-7, and D-8 was more efficient than other misincorporations in Figure 6A and possessed slightly higher substrate specificity (Table 2). These observations were possibly because dCTP skipped the template thymine base and base paired with the next template base guanine. This hypothesis is supported by the fact that Polμ causes frequent frameshift mutation *in vitro* (*15*).

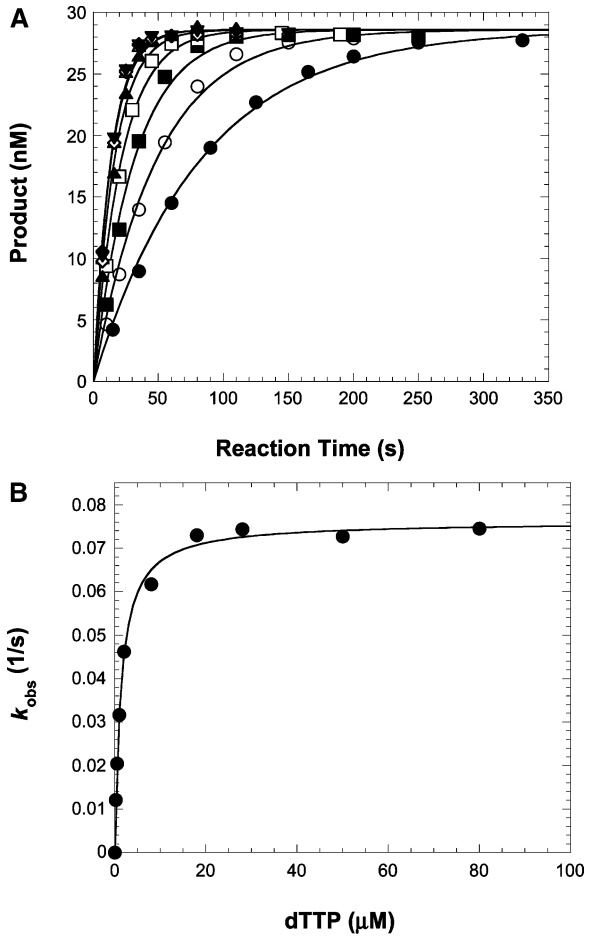

FIGURE 5: Substrate specificity of incoming correct nucleotide. (A) A preincubated solution of 30 nM D-1 and 150 nM Polμ was rapidly reacted with increasing concentrations of dTTP (0.25 μM, ●; 0.50 μM, ○; 1 μM, ■; 2 μM, □; 8 μM, ▲; 18 μM, △; 28 μM, ◆; 50 μM, ◇; 80 μM, ▼) for various time intervals. The reactions were stopped by 0.37 M EDTA. A single-exponential fit yields a k_{obs} for each dTTP concentration. (B) A hyperbolic fit of the dTTP concentration versus k_{obs} yields a K_d of 1.4 ± 0.1 and a k_p of 0.076 ± 0.001 s^{-1}.

The fidelity, defined as $(k_p/K_d)_{incorrect}/[(k_p/K_d)_{correct} + (k_p/K_d)_{incorrect}]$, was calculated for all 16 possible nucleotide incorporations (Table 2). Thus, the fidelity of dNTP polymerization catalyzed by human DNA Polμ was determined to be $10^{-4}-10^{-5}$ with normal primer/template DNA substrates. Because Polμ does not possess 3′→5′ exonuclease activity, this enzyme is thereby considered to be a low-fidelity DNA polymerase.

Substrate Specificity of Incoming Matched rNTP. TdT, the homologue of Polμ, has been previously shown to incorporate both dNTPs and rNTPs (*34*, *35*). To evaluate if Polμ possesses similar activity, we performed single matched rNTP incorporation into D-8, and the elongation of the DNA primer indicated that Polμ has RNA polymerase activity (Figure 6B). Similar results were obtained with D-1, D-6, and D-7 (data not shown). However, consecutive incorporations of rNTPs were very slow in the presence of all rNTPS (Figure 6B). These results have been observed previously by others (*16*, *17*). Additionally, misincorporations of rNTPs into D-8 (Figure 6B) were much less efficient than the misincorporations of dNTPs (Figure 6A). Thus, only matched rNTPs were kinetically competent enough to compete against dNTPs in the elongation of a DNA primer/template substrate by Polμ. The substrate specificity of each mismatched rNTP was therefore not measured.

To determine the sugar selectivity of Polμ, we measured the substrate specificity (Table 2) of each of the four matched rNTPs using assays similar to those described above. For example, Figure 7 shows that Polμ incorporated rGTP into D-8 with an equilibrium dissociation constant (K_d) of 45 ± 7 μM and a maximum rate of polymerization (k_p) of 0.000220 ± 0.000008 s^{-1}. The fidelity of misincorporations of matched rNTPs into DNA primer/template substrates was calculated to be in the range of $10^{-3}-10^{-5}$ (Table 2). Notably, the pyrimidines, especially CTP, had higher substrate specificities than the purines (Table 2). The preference was probably due to the next template base guanine, which base paired with the pyrimidines to form the second base pairs G:C or G:U (wobble). Interestingly, the incorporation efficiency (k_p/K_d) of rNTPs was higher than or similar to that of mismatched dNTPs (Table 2). This suggests that Polμ misincorporates matched rNTPs at least as frequently as it misincorporates unmatched dNTPs.

Surprisingly, the sugar selectivity, defined as the ratio of the substrate specificity of a matched dNTP and a matched rNTP, $(k_p/K_d)_{dNTP}/(k_p/K_d)_{rNTP}$, was calculated to be 492, 2074, 6122, and 10959 for the incorporation of dCTP/rCTP, dTTP/UTP, dGTP/rGTP, and dATP/rATP (Table 2). These sugar selectivities are significantly higher than the previously estimated values of 1.4−11 (*16*) and 1.34−11.04 (*17*) obtained with single-nucleotide gapped DNA substrates.

Weak Strand-Displacement Activity. To probe if Polμ possesses strand-displacement activity, we performed the incorporation of single dNTP or all four dNTPs into a single-nucleotide gapped DNA D-8g (Table 1). The multiple incorporations in the presence of all dNTPs (Figure 6C) suggested Polμ partially displaced the downstream primer 19-mer after filling the gap. This activity was not due to contamination of the primer/template 21/41-mer because the DNA was annealed with a ratio of 1:2:2 for the 21-mer:19-mer:41-mer. If there was significant amount of unwanted 21/41-mer in the reaction mixture, the product bands of 22-mer to 24-mer should not be more intense than longer product bands after 3 h of polymerization in the presence of dNTPs (Figure 6C). Small amounts of products longer than 25-mer suggested the strand-displacement activity of Polμ was relatively weak. This strand-displacement activity of Polμ was not detected by Ruiz et al. (*17*). The reason we detected this weak activity is probably due to the long reaction time and high enzyme concentration used in our studies. The energy source for this weak strand-displacement activity is probably derived from the net favorable free energy of nucleotide incorporation in addition to thermal breathing of the base pairs. The slow nucleotide incorporation by Polμ and fast DNA dissociation result in inefficient polymerization and little favorable free energy, which leads to weak strand-displacement activity.

Distributive Elongation of a Primer/Template Substrate. The kinetic studies shown in Figure 4 demonstrated Polμ has a much higher DNA dissociation rate constant than single-nucleotide incorporation rate constant, suggesting Polμ is a distributive polymerase as observed previously (*1*, *2*, *17*). To provide further evidence for this conclusion, a preincubated solution of radiolabeled D-8 and Polμ in buffer M was reacted with a solution of dNTPs in buffer M

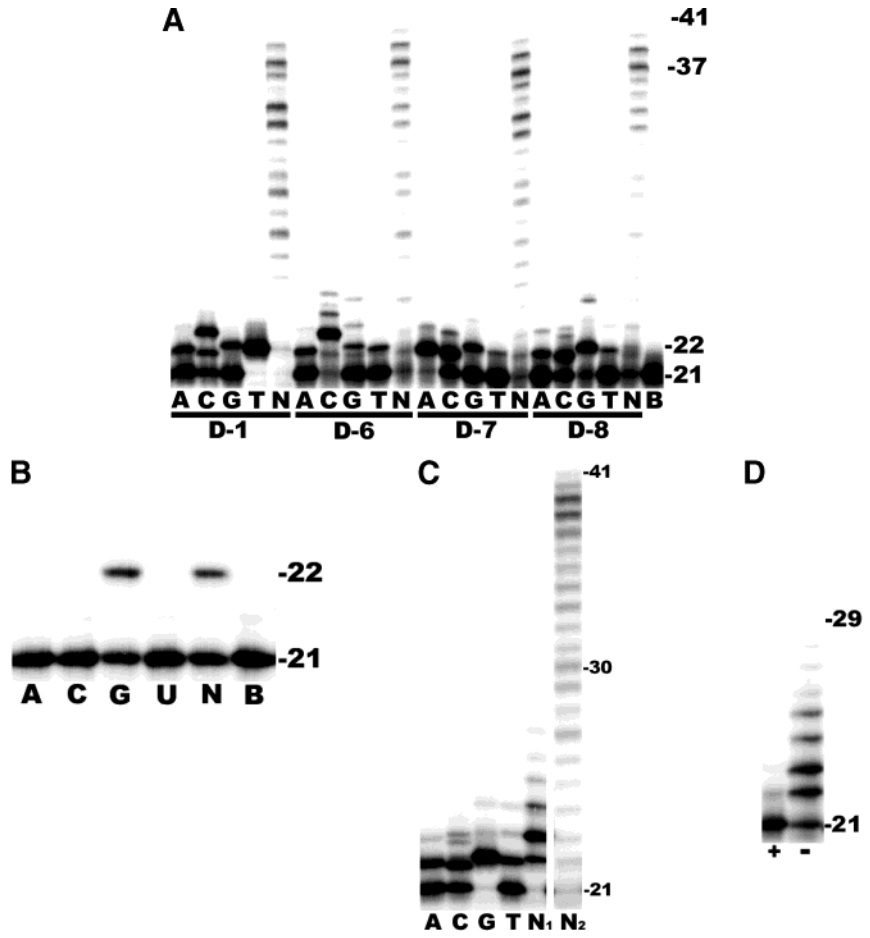

FIGURE 6: Deoxynucleotide and ribonucleotide incorporations under different reaction conditions. (A) dNTP incorporation. DNA substrates D-1, D-6, D-7, and D-8 (30 nM each) preincubated with Polμ (150 nM) were mixed with 150 μM dATP (lanes A), 150 μM dCTP (lanes C), 150 μM dGTP (lanes G), 150 μM dTTP (lanes T), 4 $\times$ 150 μM dNTPs (lanes N), and no dNTP (lane B) as indicated for 3 h. (B) rNTP incorporation. A preincubated solution of Polμ (150 nM) and D-8 (30 nM) were mixed with 150 μM rATP, 150 μM rCTP, 150 μM rGTP, 150 μM rUTP, 4 $\times$ 150 μM rNTPs (lane N), and no rNTPs (lane B) as indicated for 3 h. (C) dNTP incorporation into a single-nucleotide gapped DNA substrate D-8g. Strand displacement activity of Polμ was assessed by reacting 100 μM dATP, 100 μM dCTP, 100 μM dGTP, 100 μM dTTP, and 4 $\times$ 100 μM dNTPs (lane N_1) with a preincubated solution containing D-8g (30 nM) and Polμ (150 nM). As a control, a nongapped D-8 substrate reacted with 4 $\times$ 100 μM dNTPs was indicated in lane N_2. All reactions were quenched after 3 h. (D) DNA trap assay. Preincubated Polμ (100 nM) and D-8 (100 nM) were mixed with dNTPs (100 μM each) in the presence (+) or absence (−) of 2.44 mg/mL activated calf thymus trap DNA for 30 min.

containing a high concentration of activated calf thymus DNA (see Materials and Methods). If D-8 dissociated rapidly from Polμ, any dissociated Polμ molecules would be trapped by the large molar excess of calf thymus DNA molecules, leading to no product formation. Conversely, in the case of a slow DNA dissociation, the primer 21-mer should be elongated to longer products. Our results shown in Figure 6D qualitatively demonstrated that DNA dissociation from Polμ was relatively fast. In fact, product 22-mer was barely seen after 30 min of incubation in the presence of the trap, in contrast to the extensive product formation pattern in the absence of the trap.

DISCUSSION

To evaluate the hypothesis that human DNA polymerase μ acts as a mutase involved in somatic hypermutation (*2*), we overexpressed and purified this polymerase and determined its fidelity with the incorporations of both deoxynucleotides and ribonucleotides using pre-steady-state kinetic methods under single-turnover conditions. Polμ was found to be sensitive to temperature (Figure 3), pH, and concentrations of Mg^{2+} and salt (Figure 2). This suggests that precautions should be taken when Polμ is studied *in vitro*.

Inefficient Polymerization. The substrate specificity (0.008−0.064 μM^{-1} s^{-1}) for correct dNTP incorporations by Polμ (Table 2) is more than 1000-, 100-, and 10-fold lower than that of T7 DNA polymerase (a replicative polymerase) (*36*), Polβ (a repair polymerase) (*37*), and yeast DNA polymerase η (a DNA lesion bypass polymerase) (*27*), respectively. Moreover, the correct nucleotide incorporation rates (0.006−0.076 s^{-1}) of Polμ fall into the range of misincorporation rates by other DNA polymerases. These results suggest Polμ is a very inefficient DNA polymerase in the elongation of a primer/template substrate. It is possible that Polμ has higher polymerase activity with different types of DNA substrates. Nick McElhinny and Ramsden have found that Polμ has a >100-fold higher polymerase activity with single-nucleotide gapped DNA substrates, for example, D-8g (Table 1), than with DNA primer/template substrates (*16*). Alternatively, Polμ could interact with other proteins through its N-terminal BRCT domain, causing an increase in its polymerase activity and stability. Polμ has been found to associate with Ku and

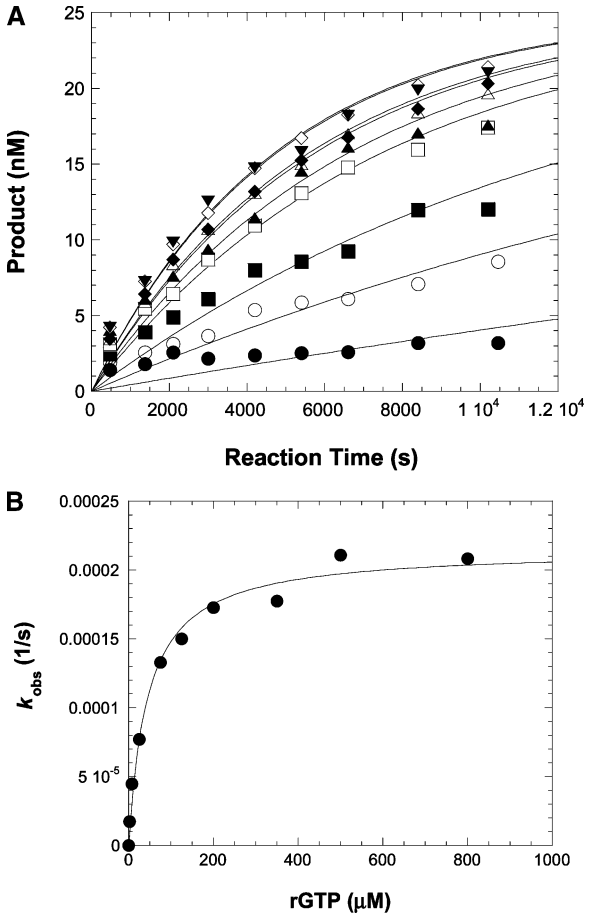

FIGURE 7: Substrate specificity of incoming correct ribonucleotide. (A) Increasing concentrations of rGTP (2 μM, ●; 8 μM,; 25 μM, ■; 75 μM, □; 125 μM, ▲; 200 μM, △; 350 μM, ◆; 500 μM, ◇; 800 μM, ▼) were rapidly mixed with a solution of preincubated D-8 (30 nM) and Polμ (150 nM). Reactions were quenched at various time increments with 0.37 M EDTA. A single-exponential fit yields a k_{obs} for each rGTP concentration. (B) A hyperbolic fit of each rGTP concentration versus the corresponding k_{obs} yields a K_d of 45 ± 7 and a k_p of 0.000220 ± 0.000008 s^{-1}.

Ligase IV *in vitro* (*14*). We are currently examining the effects of other proteins including proliferating cell nuclear antigen (PCNA) and single-nucleotide gapped DNA and on the polymerase activity of Polμ.

Fidelity of Deoxynucleotide Incorporation. The deoxynucleotide incorporation fidelity of Polμ was determined to be in the range of $10^{-4}-10^{-5}$ with DNA primer/template substrate. This range was different from the fidelity ($10^{-2}-10^{-5}$) estimated by Zhang et al. using DNA primer/template substrates and steady-state kinetic methods (*15*). The difference in the fidelity is predominantly due to the difficulty in the implementation of steady-state kinetic methods by Zhang et al. (*15*), although different DNA substrates and different reaction temperatures [25 °C in our studies versus 30 °C in their studies (*15*)] may have contributed. Zhang et al. (*15*) used 50 fmol of DNA substrate and a relatively significant amount of Polμ (14 fmol) in order to observe enough products. The enzyme/DNA substrate ratio (28%) they have used is too high to maintain bona fide steady-state reaction conditions, and the constants they have used to define the fidelity are not true steady-state kinetic parameters. The fidelity Zhang et al. estimated is thus inaccurate. Moreover, the "steady-state" kinetic parameters for several misincorporations are not reported by Zhang et al. (*15*), probably due to extremely slow product formation even under compromised steady-state reaction conditions. Therefore, the single-turnover method used in our studies has a clear advantage over steady-state kinetic methods, particularly in the studies of a slow enzyme such as Polμ (*22*).

In addition, the fidelity and substrate specificity of Polμ (Table 2) are not sequence-dependent. The asymmetry of misincorporation efficiency, for example, G:A and A:G base pairs, previously observed with Polβ (*37*) was not found (Table 2).

Overall Fidelity, Sugar Selectivity, and Ribonucleotide Incorporation. During the course of this study, two other groups (*16*, *17*) have reported the incorporation of rNTPs by Polμ, which is consistent with our results shown in Figure 6B. Surprisingly, Polμ incorporates matched CTP, UTP, and GTP more efficiently than mismatched dNTPs (Table 2). Moreover, higher cellular concentrations of rNTPs over dNTPs *in vivo* will further increase the misincorporation frequency of matched rNTPs. Thus, for any DNA polymerases that are capable of incorporating rNTPs, the fidelity evaluation should include the incorporations of both dNTPs and rNTPs. On the other hand, the incorporations of mismatched rNTPs are much less efficient than those of the matched rNTPs (Figure 6B), suggesting these types of misincorporations are rare and may not need to be considered. Together, our data in Table 2 suggest the overall fidelity of nucleotide incorporation into a DNA primer/template by Polμ is in the range of $10^{-3}-10^{-5}$. However, further extension of an incorporated rNTP with either dNTPs (*17*) or rNTPs (Figure 6B and ref *17*) is very slow, leading to arrest of DNA synthesis.

Surprisingly, the sugar selectivity of Polμ with DNA primer/template substrate, 492−10959 (Table 2), is similar to that of *E. coli* DNA polymerase I (*38*, *39*), but much larger than the selection factors previously obtained with single-nucleotide gapped DNA substrates, 1.4−11 (*16*) and 1.34−11.04 (*17*). Sequence alignment analysis coupled with site-directed mutagenesis has been used to identify amino acid residue Gly433 as being essential for Polμ to incorporate rNTPs into single-nucleotide gapped DNA. This is because the small side chain of Gly433 in motif A, unlike its counterpart Tyr271 in Polβ and Tyr505 in Polλ, does not act as a steric barrier for the 2′-OH of an incoming rNTP (*17*). Our results suggest the sugar selection by Polμ utilizes different structural mechanisms with gapped and nongapped DNA substrates. With a primer/template substrate, a residue other than Gly433 uses its bulky side chain to block the binding of the 2′-hydroxyl of an incoming rNTP. This further suggests the active site structure of Polμ is different in the presence of gapped or nongapped DNA substrates. The interaction between the downstream primer and Polμ most likely contribute to the structural change.

Comparison to Polβ. Polβ, an X-family DNA polymerase, has been well characterized by pre-steady-state kinetics (*37*, *40*−*42*). In comparison to Polβ, Polμ has a 200−500-fold slower nucleotide incorporation rate (k_p), a 20−60-fold higher nucleotide binding affinity, and an 8−25-fold lower substrate specificity (k_p/K_d) for correct dNTP incorporation into primer/template DNA substrates (Table 3). Polμ has a 100−400-fold slower polymerization rate, a 7−25-fold higher affinity,

Table 3: Comparison of Kinetic Parameters of Human Polμ and Rat Polβ with dNTP

	Polμ (primer/template DNA)		Polβ (primer/template DNA)[a]		Polβ (1 nt gapped DNA)[b]	
	correct	incorrect	correct	incorrect	correct	incorrect
K_d (μM)	0.35−1.8	7.3−135	6.7−66	181−980	1.9−8.5	190−1600
k_p (s^{-1})	0.006−0.076	(2−30) × 10^{-5}	3−17	0.008−0.03	12−36	0.019−1.3
k_p/K_d (μM^{-1} s^{-1})	0.008−0.064	(4−61) × 10^{-7}	0.2−0.5	(8−100) × 10^{-6}	4−6	(7−250) × 10^{-5}
fidelity[c]	10^{-4}−10^{-5}		10^{-4}−10^{-5}		10^{-4}−10^{-5}	

[a] Reference *37*. [b] Reference *40*. [c] Calculated as $(k_p/K_d)_{incorrect}/[(k_p/K_d)_{correct} + (k_p/K_d)_{incorrect}]$.

and a 16−20-fold lower efficiency than Polβ in the incorporations of mismatched incoming dNTPs (Table 3). Thus, Polβ is more efficient than Polμ in the incorporations of both correct and incorrect nucleotides. As a consequence of the aforementioned factors, the fidelity of Polμ and Polβ with DNA primer/template substrates is in the same range of 10^{-4}−10^{-5} (Table 3). Similarly, Polβ has higher substrate specificity in the incorporations of both correct and incorrect dNTPs with single-nucleotide gapped DNA substrates than with normal DNA substrates, but the fidelity, in comparison, is unchanged (Table 3). The different kinetic results of the two related X-family polymerases are difficult to explain structurally in the absence of a crystal structure of the ternary complex of Polμ, DNA, and an incoming nucleotide. On the basis of the high-resolution crystal structures of the ternary complexes of Polβ (*43*, *44*) and the sequence alignment analysis (*9*, *10*), we speculate that the three conserved active site residues (D330, D332, and D418) of Polμ are not positioned to be as catalytically efficient as those in Polβ (D190, D192, and D256) or that the 3′-hydroxyl of a primer is not properly aligned to attack the α-phosphate group of an incoming nucleotide. The extra N-terminal BRCT domain of Polμ may also regulate its activity because the deletion of this domain completely abolished the polymerase activity of this enzyme (S. Sompalli and Z. Suo, unpublished results). The similar fidelities of Polμ and Polβ can be explained on the basis of the fact that two of the three residues involved in nucleotide selection in Polβ (R183, F272, and G274) are conserved in Polμ (R323, W434, and G436) (*9*). Because Polμ binds both correct and incorrect nucleotides with higher affinity than Polβ (Table 3), additional residues of Polμ may also be involved in the binding of an incoming nucleotide. The different enzymatic activities of Polμ and Polβ should parallel their different biological functions. As a base excision repair enzyme, Polβ is required to be an efficient DNA polymerase with reasonably high fidelity. In contrast, Polμ may predominantly function to protect the coding ends from exonucleolytic attack during V(D)J recombination using its DNA-binding and protein−protein interaction abilities, rather than utilizing its inefficient polymerase activity (*45*) (see discussion below).

Biological Functions of Human DNA Polμ in Ig Development. V(D)J recombination and somatic hypermutation are two essential mechanisms for generating antibody diversity during human Ig development. The latter mechanism introduces an estimated 10^{-3}−10^{-4} point mutations (per base pair per generation) into the V domain of Ig genes and is essential for the affinity maturation of antibodies (*46*−*48*). The somatic hypermutation rate is ∼10^6-fold higher than the spontaneous mutation rate of the rest of the human genome. The dominant point mutations in the V domain are transition mutations at the G:C base pairs embedded in the motif of purine-G-pyrimidine-(A/T) and short palindromes or hairpin loops (*46*−*48*). The error-prone mutase involved in somatic hypermutation has not been identified despite extensive searches. Human DNA Polμ has been proposed to be the mutase based on the following characteristics: shares similar sequence (41% identity) and domain organization with TdT, one of the key proteins in V(D)J recombination; catalyzes a random insertion of nucleotides in the presence of Mn^{2+}; and is preferentially expressed in peripheral lymphoid tissues (*2*). However, this hypothesis is not supported by the inefficiency of Polμ as a polymerase (see above discussion) and its relatively high dNTP incorporation fidelity (10^{-4}−10^{-5}) (Table 2). The sequence-independent fidelity of Polμ is not consistent with the distinctive pattern of somatic hypermutation. Moreover, the fact that human Polμ catalyzes frameshift DNA synthesis with an unprecedented high frequency does not support Polμ as a mutase either (*15*).

However, more studies are required to evaluate this mutase hypothesis because both the fidelity and activity of Polμ can be affected by the identity of the metal ion cofactor and the type of DNA substrates (i.e., nongapped versus gapped). Although the metal ion cofactor for Polμ is most likely to be Mg^{2+} *in vivo* as observed with other polymerases, this has not been experimentally confirmed. If the metal ion were Mn^{2+} or Co^{+}, the fidelity of Polμ would be lower because these transition metal ions are mutagenic (*49*−*51*). For example, human Polμ has been found to incorporate more noncanonical ribonucleotides with Mn^{2+} than with Mg^{2+} (*17*). Thus, it is important to identify the metal ion cofactor for Polμ. Additionally, if the mismatch extension fidelity of Polμ is low, it could decrease the overall fidelity of this polymerase and thereby substantiate the mutase hypothesis. We are currently measuring the mismatch extension fidelity of Polμ.

Recent *in vivo* analysis of Polμ-deficient mice suggests Polμ is a key element contributing to the relative homogeneity in size of light chain CDR3 and taking part in Ig κ light chain rearrangement at a stage where TdT is no longer expressed (*45*). Polμ has also been shown to associate with Ku and XRCC4-ligase IV proteins, which are key players in NHEJ and V(D)J recombination (*14*). These results clearly demonstrate that Polμ is involved in Ig development. If Polμ is not the mutase and does not act as TdT in the presence of Mg^{2+} (*15*, *52*), it may just bind and protect coding ends from degradation by exonucleases during V(D)J recombination as proposed by Bertocci et al. (*45*). The inefficient polymerase activity (see above discussion) of Polμ somewhat supports this hypothetical role, but the relatively low DNA binding affinity revealed by Figure 4 does not. It is possible Polμ binds DNA more tightly in the presence of a nucleotide because they may form a tightly bound ternary comples, E′·DNA_n·dNTP, as has been observed in other

polymerases (*26*−*28*, *30*−*33*, *53*, *54*). Moreover, gapped DNA substrates are likely the intermediates during NHEJ and V(D)J recombination and Ig class switching. Polμ has much higher activity with short gapped DNA substrates than regular primer/template DNA substrates (*16*). This property and its ubiquitous expression in various tissues (*9*) as well as its interaction with Ku and XRCC4-ligase IV (*14*) suggest Polμ may also play a role in NHEJ. More experiments are required to clearly define the biological functions of Polμ.

REFERENCES

1. Aoufouchi, S., Flatter, E., Dahan, A., Faili, A., Bertocci, B., Storck, S., Delbos, F., Cocea, L., Gupta, N., Weill, J. C., and Reynaud, C. A. (2000) Two novel human and mouse DNA polymerases of the polX family, *Nucleic Acids Res. 28*, 3684−3693.
2. Dominguez, O., Ruiz, J. F., Lain de Lera, T., Garcia-Diaz, M., Gonzalez, M. A., Kirchhoff, T., Martinez, A. C., Bernad, A., and Blanco, L. (2000) DNA polymerase mu (Pol mu), homologous to TdT, could act as a DNA mutator in eukaryotic cells, *EMBO J. 19*, 1731−1742.
3. Wilson, S. H. (1998) Mammalian base excision repair and DNA polymerase beta, *Mutat Res. 407*, 203−215.
4. Wood, R. D., and Shivji, M. K. (1997) Which DNA polymerases are used for DNA-repair in eukaryotes? *Carcinogenesis 18*, 605−610.
5. Garcia-Diaz, M., Dominguez, O., Lopez-Fernandez, L. A., de Lera, L. T., Saniger, M. L., Ruiz, J. F., Parraga, M., Garcia-Ortiz, M. J., Kirchhoff, T., del Mazo, J., Bernad, A., and Blanco, L. (2000) DNA polymerase lambda (Pol lambda), a novel eukaryotic DNA polymerase with a potential role in meiosis, *J. Mol. Biol. 301*, 851−867.
6. Garcia-Diaz, M., Bebenek, K., Kunkel, T. A., and Blanco, L. (2001) Identification of an intrinsic 5′-deoxyribose-5-phosphate lyase activity in human DNA polymerase lambda: a possible role in base excision repair, *J. Biol. Chem. 276*, 34659−34663.
7. Kobayashi, Y., Watanabe, M., Okada, Y., Sawa, H., Takai, H., Nakanishi, M., Kawase, Y., Suzuki, H., Nagashima, K., Ikeda, K., and Motoyama, N. (2002) Hydrocephalus, situs inversus, chronic sinusitis, and male infertility in DNA polymerase lambda-deficient mice: possible implication for the pathogenesis of immotile cilia syndrome, *Mol. Cell. Biol. 22*, 2769−2776.
8. Bassing, C. H., Swat, W., and Alt, F. W. (2002) The mechanism and regulation of chromosomal V(D)J recombination, *Cell. 109 (Suppl.)*, S45−S55.
9. Ruiz, J. F., Dominguez, O., Lain de Lera, T., Garcia-Diaz, M., Bernad, A., and Blanco, L. (2001) DNA polymerase mu, a candidate hypermutase? *Philos. Trans. R. Soc. London B: Biol. Sci. 356*, 99−109.
10. Reynaud, C. A., Frey, S., Aoufouchi, S., Faili, A., Bertocci, B., Dahan, A., Flatter, E., Delbos, F., Storck, S., Zober, C., and Weill, J. C. (2001) Transcription, beta-like DNA polymerases and hypermutation, *Philos. Trans. R. Soc. London B: Biol. Sci. 356*, 91−97.
11. Callebaut, I., and Mornon, J. P. (1997) From BRCA1 to RAP1: a widespread BRCT module closely associated with DNA repair, *FEBS Lett. 400*, 25−30.
12. Bork, P., Hofmann, K., Bucher, P., Neuwald, A. F., Altschul, S. F., and Koonin, E. V. (1997) A superfamily of conserved domains in DNA damage-responsive cell cycle checkpoint proteins, *FASEB J. 11*, 68−76.
13. Gellert, M. (2002) V(D)J recombination: RAG proteins, repair factors, and regulation, *Annu. Rev. Biochem. 71*, 101−132.
14. Mahajan, K. N., Nick McElhinny, S. A., Mitchell, B. S., and Ramsden, D. A. (2002) Association of DNA polymerase mu (pol mu) with Ku and ligase IV: role for pol mu in end-joining double-strand break repair, *Mol. Cell. Biol. 22*, 5194−5202.
15. Zhang, Y., Wu, X., Yuan, F., Xie, Z., and Wang, Z. (2001) Highly frequent frameshift DNA synthesis by human DNA polymerase mu, *Mol. Cell. Biol. 21*, 7995−8006.
16. Nick McElhinny, S. A., and Ramsden, D. A. (2003) Polymerase mu is a DNA-directed DNA/RNA polymerase, *Mol. Cell. Biol. 23*, 2309−2315.
17. Ruiz, J. F., Juarez, R., Garcia-Diaz, M., Terrados, G., Picher, A. J., Gonzalez-Barrera, S., Fernandez de Henestrosa, A. R., and Blanco, L. (2003) Lack of sugar discrimination by human Pol mu requires a single glycine residue, *Nucleic Acids Res. 31*, 4441−4449.
18. Zhang, Y., Wu, X., Guo, D., Rechkoblit, O., Taylor, J. S., Geacintov, N. E., and Wang, Z. (2002) Lesion bypass activities of human DNA polymerase mu, *J. Biol. Chem. 277*, 44582−44587.
19. Havener, J. M., McElhinny, S. A., Bassett, E., Gauger, M., Ramsden, D. A., and Chaney, S. G. (2003) Translesion synthesis past platinum DNA adducts by human DNA polymerase mu, *Biochemistry 42*, 1777−1788.
20. Johnson, K. A. (1986) Rapid kinetic analysis of mechanochemical adenosinetriphosphatases, *Methods Enzymol. 134*, 677−705.
21. Gutfreund, H. (1972) *Enzymes: Physical Principles*, Wiley-Interscience, New York.
22. Johnson, K. A. (1992) Transient-state kinetic analysis of enzyme reaction pathways, *The Enzymes. 20*, 1−61.
23. Fiala, K. A., Abdel-Gawad, W., and Suo, Z. (2004) Pre-steady-state kinetic studies of the fidelity and mechanism of polymerization catalyzed by truncated human DNA polymerase λ, *Biochemistry 43*, 6751−6762.
24. Wada, K., Wada, Y., Ishibashi, F., Gojobori, T., and Ikemura, T. (1992) Codon usage tabulated from the GenBank genetic sequence data, *Nucleic Acids Res. 20 (Suppl.)*, 2111−2118.
25. Boule, J. B., Johnson, E., Rougeon, F., and Papanicolaou, C. (1998) High-level expression of murine terminal deoxynucleotidyl transferase in *Escherichia coli* grown at low temperature and overexpressing argU tRNA, *Mol. Biotechnol. 10*, 199−208.
26. Fiala, K. A., and Suo, Z. (2004) Mechanism of DNA polymerization catalyzed by *Sulfolobus solfataricus* P2 DNA polymerase IV, *Biochemistry 43*, 2116−2125.
27. Washington, M. T., Prakash, L., and Prakash, S. (2001) Yeast DNA polymerase eta utilizes an induced-fit mechanism of nucleotide incorporation, *Cell 107*, 917−927.
28. Patel, S. S., Wong, I., and Johnson, K. A. (1991) Pre-steady-state kinetic analysis of processive DNA replication including complete characterization of an exonuclease-deficient mutant, *Biochemistry 30*, 511−25.
29. Zhong, X., Patel, S. S., Werneburg, B. G., and Tsai, M. D. (1997) DNA polymerase β: multiple conformational changes in the mechanism of catalysis, *Biochemistry 36*, 11891−11900.
30. Dahlberg, M. E., and Benkovic, S. J. (1991) Kinetic mechanism of DNA polymerase I (Klenow fragment): identification of a second conformational change and evaluation of the internal equilibrium constant, *Biochemistry 30*, 4835−4843.
31. Bryant, F. R., Johnson, K. A., and Benkovic, S. J. (1983) Elementary steps in the DNA polymerase I reaction pathway, *Biochemistry 22*, 3537−3546.
32. Kuchta, R. D., Benkovic, P., and Benkovic, S. J. (1988) Kinetic mechanism whereby DNA polymerase I (Klenow) replicates DNA with high fidelity, *Biochemistry 27*, 6716−6725.
33. Johnson, A. A., Tsai, Y., Graves, S. W., and Johnson, K. A. (2000) Human mitochondrial DNA polymerase holoenzyme: reconstitution and characterization, *Biochemistry 39*, 1702−1708.
34. Boule, J. B., Rougeon, F., and Papanicolaou, C. (2001) Terminal deoxynucleotidyl transferase indiscriminately incorporates ribonucleotides and deoxyribonucleotides, *J. Biol. Chem. 276*, 31388−31393.
35. Kato, K. I., Goncalves, J. M., Houts, G. E., and Bollum, F. J. (1967) Deoxynucleotide-polymerizing enzymes of calf thymus gland. II. Properties of the terminal deoxynucleotidyltransferase, *J. Biol. Chem. 242*, 2780−2789.
36. Wong, I., Patel, S. S., and Johnson, K. A. (1991) An induced-fit kinetic mechanism for DNA replication fidelity: direct measurement by single-turnover kinetics, *Biochemistry 30*, 526−537.
37. Kraynov, V. S., Werneburg, B. G., Zhong, X., Lee, H., Ahn, J., and Tsai, M. D. (1997) DNA polymerase beta: analysis of the contributions of tyrosine-271 and asparagine-279 to substrate specificity and fidelity of DNA replication by pre-steady-state kinetics, *Biochem J. 323 (Part 1)*, 103−111.
38. Astatke, M., Ng, K., Grindley, N. D., and Joyce, C. M. (1998) A single side chain prevents *Escherichia coli* DNA polymerase I (Klenow fragment) from incorporating ribonucleotides, *Proc. Natl. Acad. Sci. U.S.A. 95*, 3402−3407.
39. Joyce, C. M. (1997) Choosing the right sugar: how polymerases select a nucleotide substrate, *Proc. Natl. Acad. Sci. U.S.A. 94*, 1619−1622.

40. Ahn, J., Werneburg, B. G., and Tsai, M. D. (1997) DNA polymerase β: structure-fidelity relationship from pre-steady-state kinetic analyses of all possible correct and incorrect base pairs for wild type and R283A mutant, *Biochemistry 36*, 1100−1107.
41. Werneburg, B. G., Ahn, J., Zhong, X., Hondal, R. J., Kraynov, V. S., and Tsai, M. D. (1996) DNA polymerase β: pre-steady-state kinetic analysis and roles of arginine-283 in catalysis and fidelity, *Biochemistry 35*, 7041−7050.
42. Liu, J., and Tsai, M. D. (2001) DNA polymerase β: pre-steady-state kinetic analyses of dATPαS stereoselectivity and alteration of the stereoselectivity by various metal ions and by site-directed mutagenesis, *Biochemistry 40*, 9014−9022.
43. Pelletier, H., Sawaya, M. R., Kumar, A., Wilson, S. H., and Kraut, J. (1994) Structures of ternary complexes of rat DNA polymerase beta, a DNA template-primer, and ddCTP, *Science 264*, 1891−1903.
44. Sawaya, M. R., Prasad, R., Wilson, S. H., Kraut, J., and Pelletier, H. (1997) Crystal structures of human DNA polymerase β complexed with gapped and nicked DNA: evidence for an induced fit mechanism, *Biochemistry 36*, 11205−11215.
45. Bertocci, B., De Smet, A., Berek, C., Weill, J. C., and Reynaud, C. A. (2003) Immunoglobulin kappa light chain gene rearrangement is impaired in mice deficient for DNA polymerase mu, *Immunity 19*, 203−211.
46. Wagner, S. D., and Neuberger, M. S. (1996) Somatic hypermutation of immunoglobulin genes, *Annu. Rev. Immunol. 14*, 441−457.
47. Neuberger, M. S., and Milstein, C. (1995) Somatic hypermutation, *Curr. Opin. Immunol. 7*, 248−254.
48. Gonzalez-Fernandez, A., Gupta, S. K., Pannell, R., Neuberger, M. S., and Milstein, C. (1994) Somatic mutation of immunoglobulin lambda chains: a segment of the major intron hypermutates as much as the complementarity-determining regions, *Proc. Natl. Acad. Sci. U.S.A. 91*, 12614−12618.
49. El-Deiry, W. S., Downey, K. M., and So, A. G. (1984) Molecular mechanisms of manganese mutagenesis, *Proc. Natl. Acad. Sci. U.S.A. 81*, 7378−7382.
50. Goodman, M. F., Keener, S., Guidotti, S., and Branscomb, E. W. (1983) On the enzymatic basis for mutagenesis by manganese, *J. Biol. Chem. 258*, 3469−3475.
51. Weymouth, L. A., and Loeb, L. A. (1978) Mutagenesis during in vitro DNA synthesis, *Proc. Natl. Acad. Sci. U.S.A. 75*, 1924−1928.
52. Covo, S., Blanco, L., and Livneh, Z. (2004) Lesion bypass by human DNA polymerase mu reveals a template-dependent, sequence-independent nucleotidyl transferase activity, *J. Biol. Chem. 279*, 859−865.
53. Kati, W. M., Johnson, K. A., Jerva, L. F., and Anderson, K. S. (1992) Mechanism and fidelity of HIV reverse transcriptase, *J. Biol. Chem. 267*, 25988−25997.
54. Kuchta, R. D., Mizrahi, V., Benkovic, P. A., Johnson, K. A., and Benkovic, S. J. (1987) Kinetic mechanism of DNA polymerase I (Klenow), *Biochemistry 26*, 8410−8417.

BI048782M